

Effects of ACI and nonlinearities on the performance of differentially detected GMSK signals

P.T. Mathiopoulos, J.S. Toor and G.K. Karagiannidis

Abstract: The effects on the performance of differentially detected Gaussian minimum shift keying (GMSK) signals operated in the presence of adjacent channel interference (ACI), modulator impairments, amplifier nonlinearities and additive white Gaussian noise is investigated. By means of computer simulation, the bit error rate (BER) performance of 1- and 2-bit conventional and decision feedback differentially detected (C-DD and DF-DD) GMSK systems in the presence of static and Rayleigh faded ACI is obtained. It is found that the best performance is achieved by the 2-bit DF-DD receiver and has resulted in BER performance improvements for the static ACI channel and error floor reductions for the Rayleigh faded ACI channel. The effects on the BER performance of a cascade of imperfect GMSK quadrature modulators and a nonlinear amplifier in conjunction with the resulting ACI are also investigated. The combination of ‘typical’ and ‘extreme’ operating conditions for the modulator are considered. For all combinations, it was found that the DF-DD receivers perform better than the C-DD receivers. However, for systems operating under ‘typical’ operating conditions, the 2-bit DF-DD receiver exhibits the best performance.

1 Introduction

The adoption of Gaussian minimum shift keying (GMSK) signals [1], as the transmission standard for various wireless mobile telecommunication systems, such as the pan-European digital cellular network (GSM) [2] and the digital European cordless telecommunications (DECT) [3], has established its importance as a modulation scheme.

Among the various signal detection techniques which can be employed in conjunction with GMSK signals, decision feedback differential detection (DF-DD) has been proposed to improve the performance of conventional differentially detected (C-DD) GMSK schemes [4, 5]. Although in the past, the DF-DD technique has been considered under different operating conditions, including the additive white Gaussian noise (AWGN) channel [4], fading [5, 6], and co-channel interference (CCI) [7], so far it has not been investigated in the presence of adjacent channel interference (ACI). Despite the fact that for cellular mobile radio systems, ACI is a less problematic interference as compared to CCI, it nevertheless still represents a non-negligible source of interference and thus system performance degradation [8, 9]. Furthermore, for non-cellular types of communication systems, especially for bandwidth and power efficient frequency division multiple access (FDMA) systems, ACI is one of the prominent sources of interference (see for example [9, 10]). Additionally, an intentional increase of ACI, for example by reducing the frequency channel spacing between adjacent channels, could signifi-

cantly increase the overall spectral efficiency of the communication system under consideration [9, 11, 12]. For digital audio broadcasting (DAB) systems, such as the Eureka 147 DAB system [13], it has been noted that in the presence of ACI the outer orthogonal frequency division multiplexing (OFDM) sub-carriers are most vulnerable to corruption and the interference on the upper and lower sidebands is independent [14]. As it was pointed out in [15], ACI could also degrade the performance of digital TV (DTV) systems.

Another type of distortion that usually is not considered in constant envelope schemes, such as an ‘ideal GMSK’ signal is nonlinear distortion. (The term ‘ideal GMSK’ signal refers to an ideal, i.e. constant envelope, GMSK signal.) Such distortion is typically due to the presence of a nonlinear amplifier [16]. It is well accepted that for a constant envelope scheme, nonlinear amplification has little effect on the spectrum and the overall system performance [17]. However, hardware implementation imperfections, such as, for example, modulator deficiencies, would result in a non-constant envelope (i.e. non-ideal) GMSK signal [18]. When such a non-ideal, non-constant envelope GMSK signal is passed through a nonlinear amplifier, it results in spectral spreading and thus creates additional ACI. The effects of nonlinear amplification of other non-constant envelope signals employed in DAB and DTV broadcasting systems have been studied in [19] and [20], respectively.

Motivated by the above, we now investigate the performance of DF-DD receivers in conjunction with ideal and non-ideal GMSK signals in the presence of static and faded ACI and nonlinearities.

2 Communication system model

Following [17], the transmitted GMSK signal can be mathematically represented as:

$$s(t) = A_0 \cos[2\pi f_{ct} t + \varphi(t)] \quad (1)$$

© IEE, 2004

IEE Proceedings online no. 20040364

doi:10.1049/ip-com:20040364

Paper first received 24th September 2001 and in revised form 13th August 2003

P.T. Mathiopoulos and G.K. Karagiannidis are with the Institute for Space Applications and Remote Sensing, National Observatory of Athens, Metaxa and V. Pavlou Str., P. Pendeli, Athens GR-15236, Greece

J.S. Toor is with AT&T, Seattle, WA, USA

where A_0 is a constant amplitude, f_c is the carrier frequency and $\phi(t)$ is given by:

$$\varphi(t) = \pi \sum_l b_l \int_{-\infty}^t g(\beta - lT) d\beta \quad (2)$$

In the above equation, T is the bit duration, $g(t)$ is the impulse response of the well known Gaussian low pass filter which has a normalised 3-dB bandwidth $B_i T$, and $b_l = -a_l b_{l-1}$, where a_l are independent and equiprobable information bits taking values from the alphabet $\{\pm 1\}$. As pointed out in [4], for the 1-bit differential detector, differential encoding is not needed and thus for this case, $b_l = a_l$. Expanding (1), $s(t)$ can be expressed in an equivalent in-phase (I-) and quadrature-phase (Q-) form as:

$$s_I(t) = s_I(t) A_0 \cos(2\pi f_{ct}) - s_Q(t) A_0 \sin(2\pi f_{ct}) \quad (3)$$

where $s_I(t) = \cos[\varphi(t)]$ and $s_Q(t) = \sin[\varphi(t)]$. An ideal quadrature modulator (QM) does not introduce any signal distortion. However, in practice non-ideal components of the QM will introduce signal distortions, including signal imbalances and offsets between the I- and Q-channels. In [18], the effects of QM deficiencies on the transmitted signal have been identified as differential amplitude imbalance (Δ), local oscillator breakthrough and DC offsets (k), and differential phase error (θ_d) which can also be represented as differential time delay τ_d , with $\tau_d = 2T\theta_d/\pi$. Mathematically, it is convenient to group all these QM deficiencies together in one of the channels, e.g. the I-channel. This is illustrated in Fig. 1. Therefore, for such a non-ideal QM (NI-QM), the distorted GMSK signal $s'(t)$ can be mathematically expressed as:

$$s'(t) = \sqrt{\{k + \Delta \cos[\varphi(t - \tau_d)]\}^2 + \sin^2[\varphi(t)]} \cdot \cos\left[2\pi f_{ct} t + \tan^{-1}\frac{\sin[\varphi(t)]}{k + \Delta \cos[\varphi(t - \tau_d)]}\right] \quad (4)$$

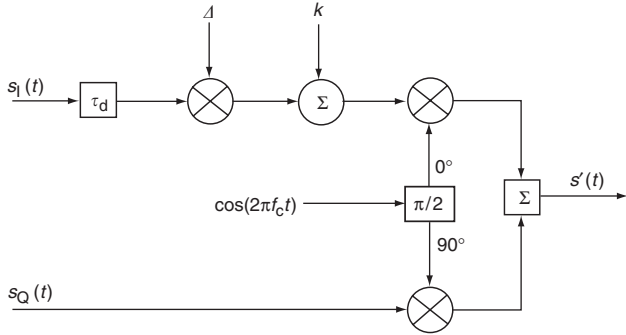


Fig. 1 Block diagram of imperfect QM

It is evident that $s'(t)$ is no longer a constant envelope scheme, except for $k=0$, $\Delta=1$ and $\tau_d=0$. Clearly, in this specific case $s'(t)=s(t)$, which is an ideal GMSK signal. Following [18], we have considered the following two sets of values for modelling the imperfections of the NI-QM:

- (i) $\theta_d=1^\circ$, $\Delta=0.95$, $k=-24$ dB ('typical values')
- (ii) $\theta_d=15^\circ$, $\Delta=0.65$, $k=-12$ dB ('extreme values').

As illustrated in Fig. 2, the NI-QM can be followed by a nonlinear amplifier (NLA). Similar to [12], we have considered a severely NLA, with the transfer function of a hard-limiter (HL) given by:

$$s''(t) = s'(t)/|s'(t)| \quad (5)$$

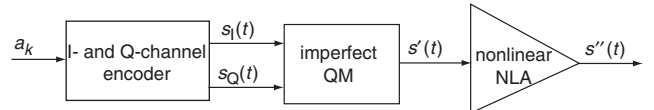


Fig. 2 GMSK transmitter employing imperfect QM and NLA

Assuming that the m th adjacent channel interferer $i_m(t)$ is of the same modulation format as $s(t)$, it can be mathematically expressed as:

$$i_m(t) = B_m \cos[2\pi(f_c + f_m)t + \theta_m + \varphi_m(t)] \quad (6)$$

where B_m is a constant amplitude, f_m is the difference in the frequency allocation of the two carriers and θ_m denotes the lack of coherence between $s(t)$ and $i_m(t)$. θ_m is assumed to be uniformly distributed over $(0, 2\pi]$. Furthermore, $\varphi_m(t)$ is given by:

$$\varphi_m(t) = \pi \sum_i c_i \int_{-\infty}^t g(\gamma - iT - \tau_m) d\gamma \quad (7)$$

where c_i are independent and equiprobable bits taking values from the alphabet $\{\pm 1\}$ and τ_m is the timing offset between $s(t)$ and $i_m(t)$. τ_m is assumed to be uniformly distributed over the time interval $(0, T]$.

Typically, there are two adjacent channel interferers who contribute most significantly to the degradation of telecommunication systems. Both of them are located in the frequency domain adjacent to the channel through which the information signal is transmitted. Assuming that both interferers are symmetrically located in the frequency domain around f_c , the carrier frequency of the upper interferer, denoted as $i^+(t)$, is $f_c + f_m$, whereas the carrier frequency of the lower interferer, denoted as $i^-(t)$, is $f_c - f_m$. In addition to the static ACI environment, we will consider the case where all three signals under consideration could be also faded by three independent but statistical identical fading signals $f^i(t)$ with $i \in \{0, \pm 1\}$. The complete channel model currently considered is illustrated in Fig. 3a, where the two switch positions indicate that we could have either a static channel (SC) or a faded channel (FC). The fading signals $f^i(t)$ have Rayleigh statistical characteristics employing the land-mobile fading model with a normalised Doppler shift of FDT [21], and are generated as discussed in [22–24].

After the addition of the WGN $n(t)$, which has a double-sided power spectral density of $N_0/2$, the received signal $r(t)$ can be expressed as:

$$r(t) = \begin{cases} s''(t) + i^+(t) + i^-(t) + n(t) & \text{for SC} \\ s''(t) + i_f^+(t) + i_f^-(t) + n(t) & \text{for FC} \end{cases} \quad (8)$$

For a linear channel, i.e. without the use of the NI-QM and NLA, $s''(t) = s(t)$ or $s''(t) = s_f(t)$. The receivers considered in this work consist of a predetection fourth-order Butterworth low-pass filter (LPF), $H_R(f)$, with a 3 dB double-sided bandwidth B_R , followed by 1- and 2-bit differential detectors with and without feedback. As previously indicated, we will be referring to these receivers as 'decision feedback differential detectors' (DD-DF) and 'conventional differential detectors' (C-DD), respectively. Their detailed structure has been previously presented in [4] and [7].

3 Performance evaluation results and discussion

The communication system described in the preceding Section was extensively evaluated by means of computer simulation using Monte Carlo error counting techniques. For all three GMSK transmitters, we have assumed that

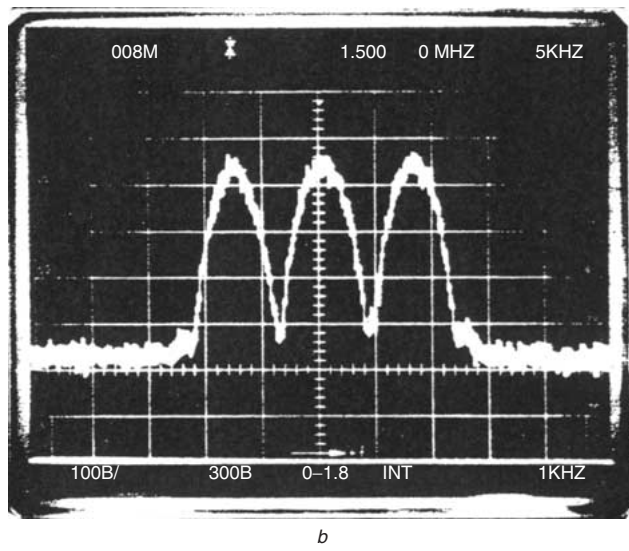
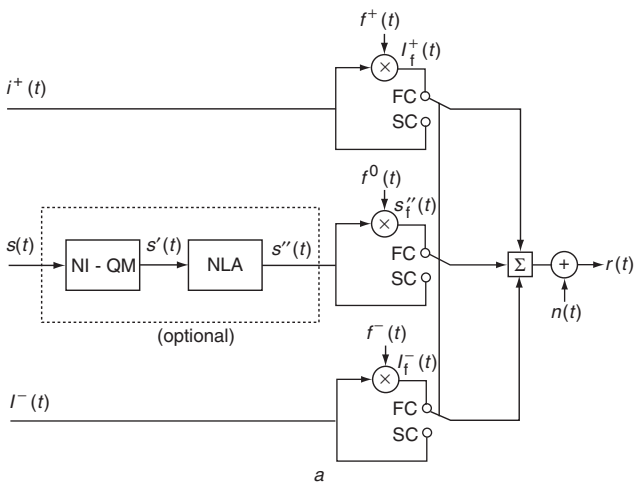


Fig. 3 The ACI model

a Detailed block diagram

b Experimental spectrum of the received signal under static ACI and AWGN conditions

$B_t T = 0.3$ as this is the specification adopted by the pan-European digital cellular network [2]. The $B_R T$ product of the predetection filter $H_R(f)$ was chosen to be 0.97 for all the receivers (with or without feedback) employing 1-bit differential detectors and 0.85 for all the receivers employing 2-bit differential detection. The reason for these choices was the near-optimal performance of the receivers for these values at a bit error rate (BER) of 10^{-3} in an AWGN channel [7]. In Fig. 3b, the experimental spectrum of the received signal in a static ACI and AWGN channel is illustrated. Details of the experimental prototype set-up, which has been employed to generate such signals and has verified some of the computer simulated results can be found in [25].

For ACI dominated applications, normally the most important parameter influencing the BER performance is the overall ACI power, which greatly depends upon the adjacent channel frequency spacing and the actual power of the interfering signals. For convenience we will assume that the interferers have the same transmitted power, i.e. $A_0 = B_1 = B_{-1}$. The carrier-to-interference ratio (C/I_A) is defined as the ratio between the average power of the desired information signal (P_{DIS}) and the average power of the adjacent interfering signals (P_{AIS}), both measured at the

output of $H_R(f)$, i.e.:

$$C/I_A = 10 \log_{10} (P_{DIS}/P_{AIS}) \quad (9)$$

For a given $B_t T$ and $B_R T$, C/I_A will be controlled by changing the spacing frequency f_m of the adjacent channels, or equivalently the adjacent channel frequency spacing normalised to the rate of transmission, $F_m = f_m T$. Clearly, the smaller F_m becomes, i.e. the closer the adjacent channel interferers are to the main channel the smaller C/I_A becomes. However, at the same time, the overall spectral efficiency is increasing. Similar to [12], here we define the spectral efficiency η as the inverse of F_m , i.e. $\eta = 1/F_m$.

In Sections 3.1 and 3.2, we will be presenting BER performance evaluation results for the linear and the nonlinear channel.

3.1 Linear channel

As illustrated in Fig. 3a, for the linear channel $s''(t) = s(t)$, i.e. the NI-QM and NLA are not present. By means of computer simulation, we have first numerically computed the value of C/I_A which is introduced as a function of F_m for both 1-bit and 2-bit DF-DD receivers. The obtained results are illustrated in Fig. 4, where we note that they are different for the two types of receivers. This is solely due to the fact that the $B_R T$ of the two types of receivers is different and clearly does not depend on the operating signal-to-noise ratio (SNR) and fading. The performance of 1- and 2-bit C-DD and DF-DD receivers was evaluated in both static (i.e. non-faded) and Rayleigh faded ACI and AWGN channels. Figure 5 illustrates the BER performance evaluation results for the static ACI at $C/I_A = 15$ dB where it is clear that the DF-DD receivers outperform the C-DD receivers. For example, at a BER of 10^{-3} , the 2-bit DF-DD receiver results in performance gains of more than 6 dB as compared to that of the equivalent 2-bit C-DD receiver. These significant performance improvements are due to the fact that the DF-DD technique increases the opening of the eye-diagram improving the detection [25]. We also note that, as compared to the 1-bit C-DD receiver, the gains for the 1-bit DF-DD receiver are even higher. Additional BER

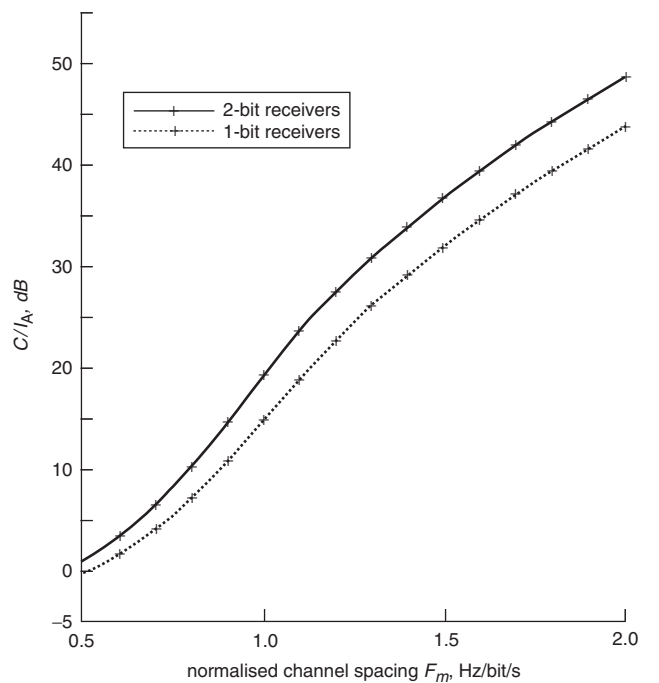


Fig. 4 Level of C/I_A as a function of normalised channel spacing F_m

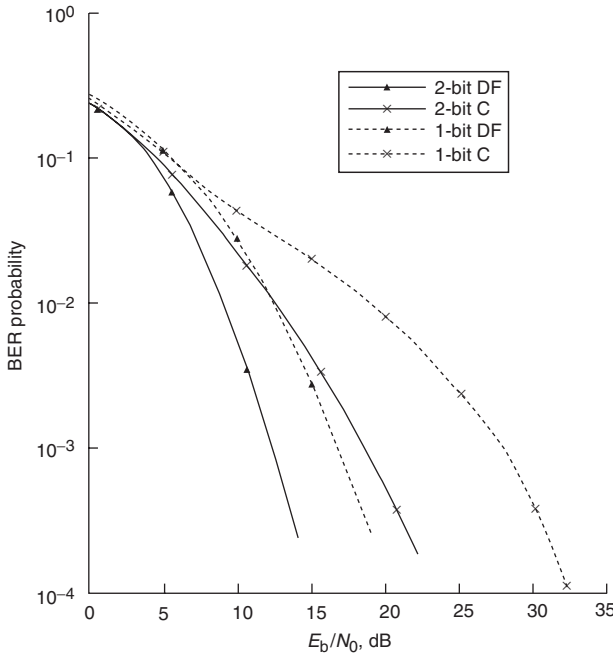


Fig. 5 BER performance of C- and DF-DD receivers at C/I_A in a static ACI-AWGN channel

performance evaluation results, which have been presented in [25], have indicated that by further increasing C/I_A , the performance gains are increasing, whereas by decreasing C/I_A , these gains are also decreasing.

Furthermore we have evaluated the degradation of E_b/N_0 (at $\text{BER} = 10^{-3}$) as a function of F_m and η for the 1-bit and 2-bit C-DD and DF-DD receivers. For all receivers, the degradation is measured with respect to the value of E_b/N_0 required by the 2-bit DF-DD to achieve a BER of 10^{-3} . The obtained performance results for the 2-bit DD receivers are summarised in Figs. 6 and 7. As expected, they indicate that for every value of the F_m , the DF-DD receivers outperform the conventional receivers. It was also found that the performance of the 2-bit DF-DD receiver is always better than that of the equivalent 1-bit DF-DD receivers. Another interesting observation is that for values of $F_m > 1.0$ (approximately), the degradation introduced by the ACI is rather small. For these values of F_m , the corresponding values of C/I_A are about 20 dB. Equivalently, by reducing F_m to about 1.0, the overall spectral efficiency is $\eta \approx 1 \text{ bit/s/Hz}$.

We have also obtained the performance of these receivers in the presence of Rayleigh faded ACI and AWGN. Similar to the other types of interference, such as for example static and faded CCI [7], the decision feedback receivers offer improvements in the performance mainly by means of reducing the error floors. A summary of the level of these error floors at various C/I_A levels and F_{DT} have been tabulated in Table 1.

3.2 Nonlinear channel

For the nonlinear channel, we assume that, as illustrated in Fig. 3a, the NI-QM and the NLA are present. Since the nonlinearities cause spectral spreading, new C/I_A as a function of F_m curves first need to be computed. It has been shown in [25], that the C/I_A curves for the non-ideal GMSK system with ‘typical’ values of QM errors are almost identical as those for the ideal GMSK system. However, for the extreme values of QM errors, these curves are noticeably different. For example, as illustrated in Fig. 7, for the 2-bit

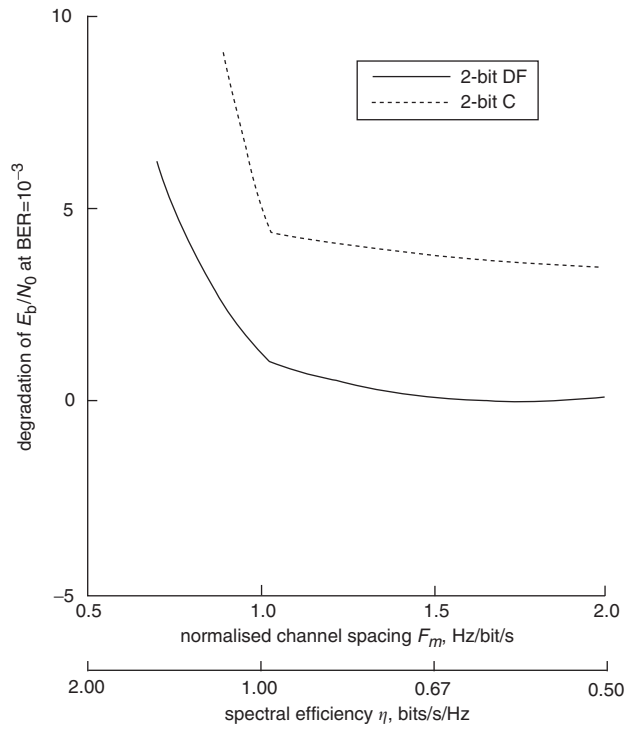


Fig. 6 Degradation of E_b/N_0 at $\text{BER} = 10^{-3}$ as a function of normalised channel spacing for 2-bit receivers in a static ACI-AWGN channel

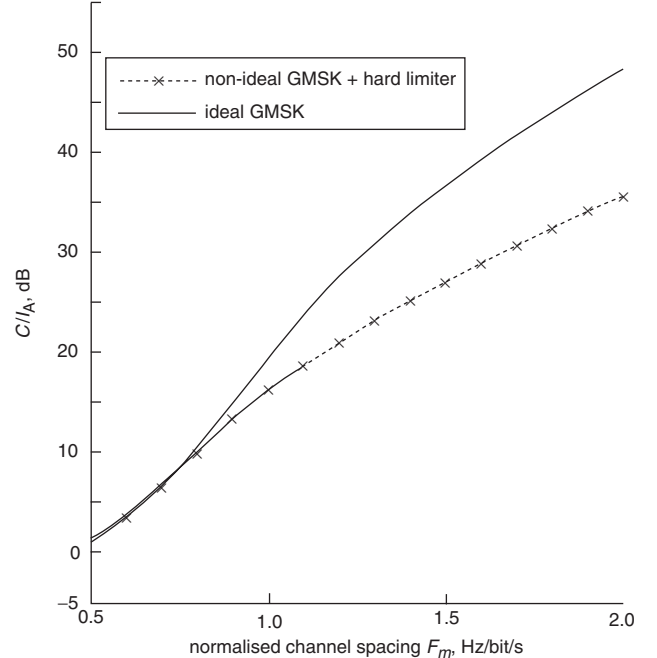


Fig. 7 C/I_A ratio as a function of normalised channel spacing (F_m) for the 2-bit receivers
QM errors are under ‘extreme conditions’, i.e. $\theta_d = 15^\circ$, $\Delta = 0.65$, $k = -12 \text{ dB}$

differential receiver and for extreme values of QM errors, C/I_A drops significantly especially when a HL is employed. This is due to the spectral spreading caused by the nature of the extreme nonlinear function of the HL [18]. Similar results have been obtained for the 1-bit differential receiver [25].

Figure 8 illustrates typical BER performances of the various differential receivers under investigation for a static

Table 1: Error floors for C- and DF-DD receivers in faded ACI and AWGN channels

$F_D T$	C/I_A , dB	Receiver type			
		1-bit C	1-bit DF	2-bit C	2-bit DF
0.03	20	0.02	0.013	0.061	0.035
0.003	20	0.0095	0.0085	0.027	0.075
0.03	30	0.013	0.008	0.055	0.03
0.003	30	0.0019	0.0014	0.004	0.0014
0.03	40	0.011	0.0075	0.005	0.03
0.003	40	0.0028	0.002	0.0011	0.0003

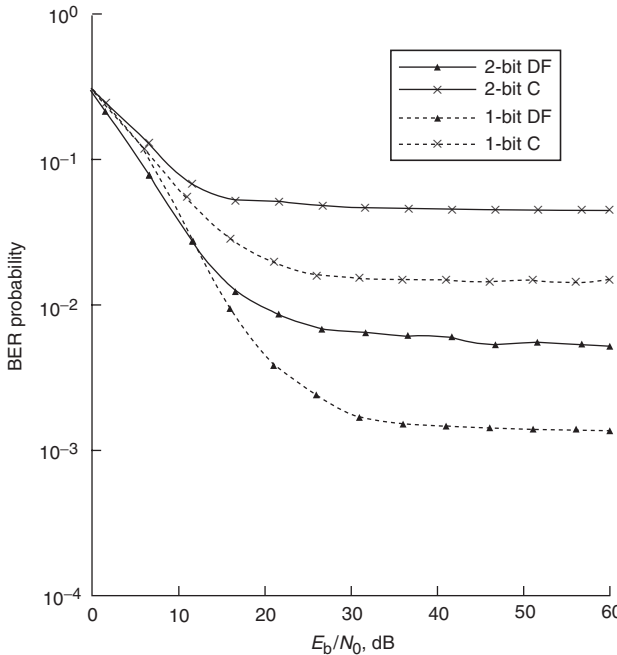


Fig. 8 BER performance of non-ideal GMSK system with conventional (C) and decision feedback (DF) receivers at $C/I_A = 15$ dB in static ACI-AWGN channel
QM errors are under ‘extreme conditions’, i.e. $\theta_d = 15^\circ$, $\Delta = 0.65$, $k = -12$ dB

ACI with $C/I_A = 15$ dB. For all systems, it has been assumed that a NI-QM with extreme values of QM errors and a HL are employed. It is clear that the DF-DD receivers perform much better than the C-DD receivers, with the 1-bit DF-DD receiver outperforming the other receivers. It is interesting to note that if C/I_A decreases, the performance limitations appear in the form of error floors and that the DF-DD receivers offer significant error floor reductions. For example, at $C/I_A = 15$ dB the 1-bit DF-DD receiver exhibits an error floor at about 1.5×10^{-3} , whereas the 1-bit C-DD receiver has an error floor at about one order of magnitude higher, i.e. of about 10^{-2} .

Figures 9–12 illustrate the degradation in E_b/N_0 (at $\text{BER} = 10^{-3}$) as a function of the normalised channel spacing F_m and equivalent spectral efficiency η . The degradation for all investigated differential receivers is measured with respect to the E_b/N_0 that is required by an ideal GMSK system employing a 2-bit DF-DD receiver to achieve a $\text{BER} = 10^{-3}$. The plots for the ideal GMSK system (i.e. without any QM errors and nonlinearities) are also included for comparison purposes. First, it is clear from

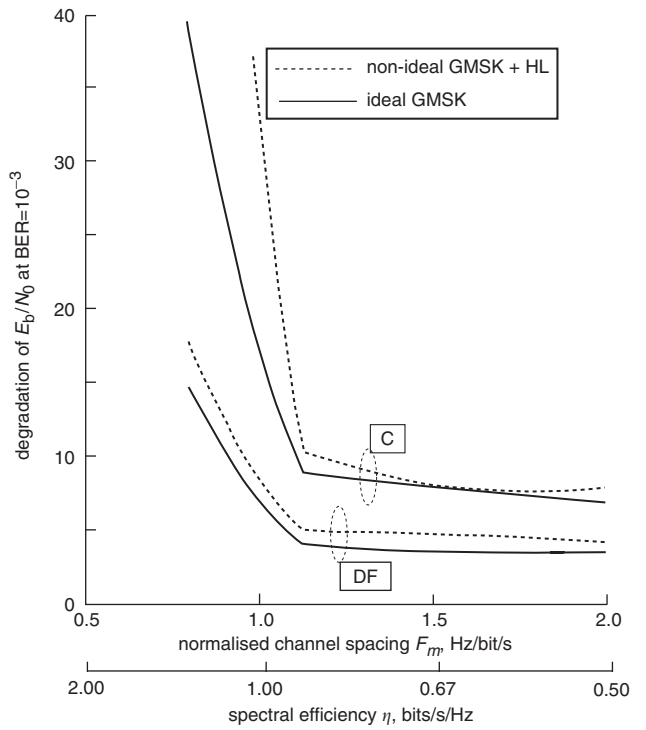


Fig. 9 E_b/N_0 degradation to achieve a $\text{BER} = 10^{-3}$ against normalised channel spacing for 1-bit conventional (C) and decision feedback (DF) receivers in a static ACI-AWGN channel under ‘typical’ QM operating conditions

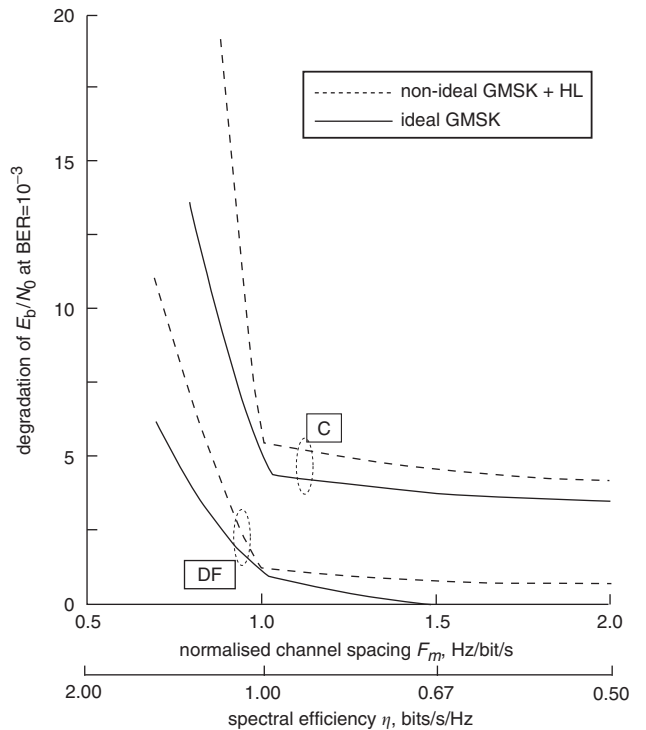


Fig. 10 E_b/N_0 degradation to achieve a $\text{BER} = 10^{-3}$ against normalised channel spacing for 2-bit conventional (C) and decision feedback (DF) receivers in a static ACI-AWGN channel under ‘typical’ QM operating conditions
 $\theta_d = 1^\circ$, $\Delta = 0.95$, $k = -24$ dB

these simulation results that the DF-DD receivers outperform the C-DD receivers for all channel conditions considered. It is also interesting to note that in all graphs there is a value of F_m below which the required E_b/N_0 to

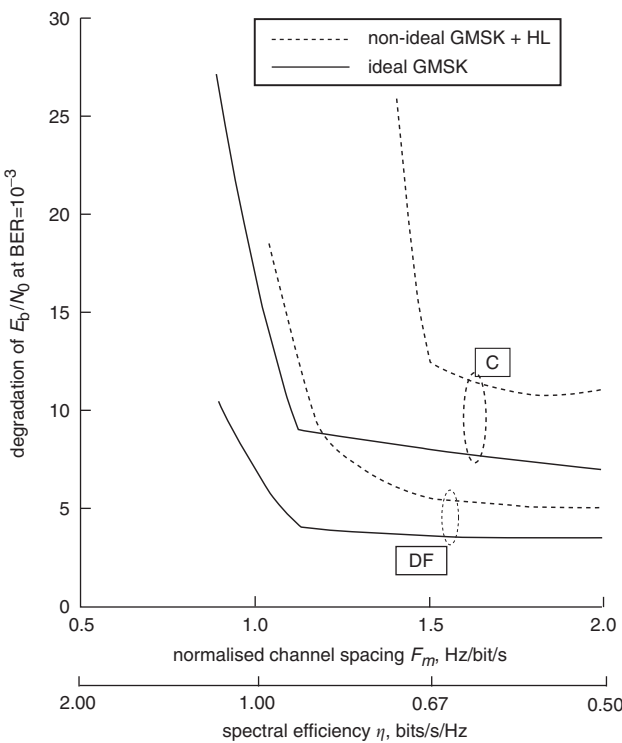


Fig. 11 E_b/N_0 degradation to achieve a BER of 10^{-3} against normalised channel spacing for 1-bit conventional (C) and decision feedback (DF) receivers in a static ACI-AWGN channel under ‘extreme’ QM operating conditions
 $\theta_d = 15^\circ$, $\Delta = 0.65$, $k = -12$ dB

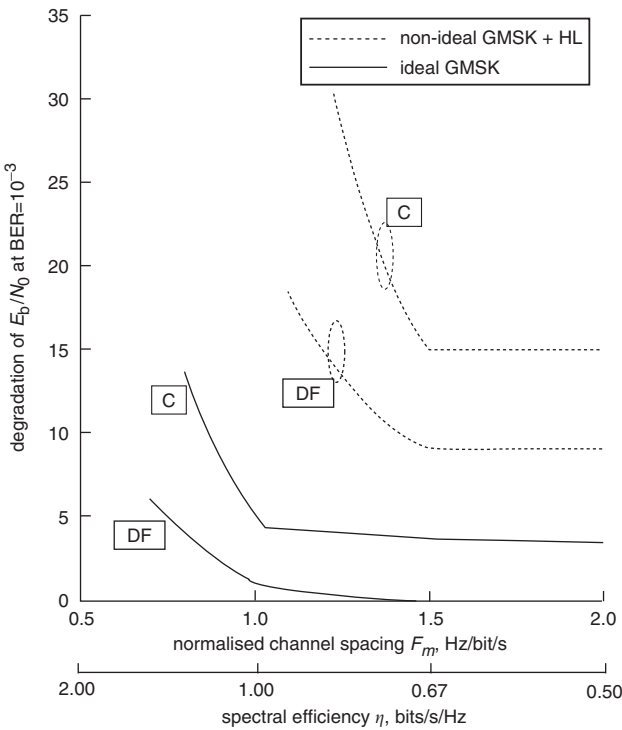


Fig. 12 E_b/N_0 degradation to achieve a BER of 10^{-3} against normalised channel spacing for 2-bit conventional (C) and decision feedback (DF) receivers
 $\theta_d = 15^\circ$, $\Delta = 0.65$, $k = -12$ dB

achieve a BER of 10^{-3} increases significantly. We will be referring to this value of F_m as F_m^c . This rather sharp increase in degradation at F_m^c is due to the rapidly increasing amount of ACI resulting from the narrowband spectra

($B_t T = 0.3$) of both useful and interfering GMSK signals. Figures 9 and 10 illustrate performance evaluation results for the case where ‘typical’ values of the QM errors are present. From these Figures it can be observed that the degradations caused by the nonlinear channel (i.e. QM errors and the NLAs) are relatively small (≈ 1 dB) when $F_m > F_m^c$. However, when $F_m < F_m^c$, the degradation caused by the nonlinearities are much higher for the C-DD receivers than the equivalent degradations for the DF-DD receivers.

For the case of extreme values of the QM errors, as illustrated in Figs. 11 and 12, F_m^c for the C-DD receivers is much higher than the equivalent F_m^c of the DF-DD receivers. For example, as it can be seen from Fig. 12, when a HL is employed, $F_m^c \approx 1.25$ (for the 1-bit DF-DD receiver) and $F_m^c \approx 1.5$ (for the 1-bit C-DD receiver). If we view F_m^c as an absolute minimum F_m at which the system can operate with satisfactory performance, then clearly the systems employing DF-DD receivers will allow narrow channel spacing. In this sense, a higher spectral efficiency can be also achieved by these decision feedback communication systems. It should be noted that by employing more advanced receiver structures, e.g. similar to those reported in [23], further improvements of the performance are expected.

4 References

- Murota, K., and Hirade, K.: ‘GMSK modulation for digital mobile radio telephony’, *IEEE Trans. Commun.*, 1981, **29**, (7), pp. 1044–1050
- Goodman, D.J.: ‘Second generation of wireless information networks’, *IEEE Trans. Veh. Technol.*, 1991, **40**, (2), pp. 366–371
- ETSI: ‘Digital European Cordless Telecommunications - Common Interface, Radio Equipment and Systems’ Valborne, France, 1990
- Yongacoglu, A., Makrakis, D., and Feher, K.: ‘Differential detection of GMSK using decision feedback’, *IEEE Trans. Commun.*, 1988, **36**, (6), pp. 641–648
- Adachi, F., and Ohno, K.: ‘Performance analysis of GMSK frequency detection with decision feedback equalisation in digital land mobile radio’, *IEE Proc., Comput. Digit. Tech.*, 1988, **135**, (6), pp. 199–207
- Korn, I.: ‘GMSK with differential phase detection in the satellite mobile channel’, *IEEE Trans. Commun.*, 1990, **38**, pp. 1980–1986
- Shin, S.S., and Mathiopoulos, P.T.: ‘Differentially detected GMSK signals in CCI channels for mobile cellular telecommunication systems’, *IEEE Trans. Veh. Technol.*, 1993, **42**, (3), pp. 289–293
- Lee, W.C.Y.: ‘Mobile cellular telecommunications’ (McGraw-Hill, New York, USA, 1995, 2nd edn.)
- Golestaneh, S., Hafez, H.M., and Mahmoud, S.A.: ‘The effects of adjacent channel interference on the capacity of FDMA cellular systems’, *IEEE Trans. Veh. Technol.*, 1994, **43**, (4), pp. 946–954
- Milstein, L.B., Pickholtz, R.L., and Schilling, D.L.: ‘Comparison of performance of digital modulation techniques in the presence of adjacent channel interference’, *IEEE Trans. Commun.*, 1982, **30**, (8), pp. 1984–1993
- Korn, I.: ‘Differential phase shift keying in two-path Rayleigh channel with adjacent channel interference’, *IEEE Trans. Veh. Technol.*, 1991, **40**, (2), pp. 461–471
- Le-Ngoc, T., and Feher, K.: ‘Performance of IJF-OQPSK modulation schemes in a complex interference environment’, *IEEE Trans. Commun.*, 1983, **31**, (1), pp. 137–144
- Thibault, L., and Le, M.T.: ‘Performance evaluation of COFDM for digital audio broadcasting – Part I: Parametric study’, *IEEE Trans. Broadcast.*, 1997, **43**, (1), pp. 64–75
- Kroeger, B., and Cammarata, D.: ‘Robust modem and coding techniques for FM hybrid IBOC DAB’, *IEEE Trans. Broadcast.*, 1997, **43**, (4), pp. 412–420
- Eilers, C., and Sgrignoli, G.: ‘Analyzing the FCC’s DTV spectral emission mask and potential degradation to adjacent channel interference due to antenna pattern differences’, *IEEE Trans. Broadcast.*, 1998, **44**, (1), pp. 28–39
- Ariyavitsakul, S., and Liu, T.: ‘Characterizing the effects of nonlinear amplifiers on linear modulation for portable radio’, *IEEE Trans. Veh. Technol.*, 1990, **39**, (4), pp. 383–389
- Sunberg, C.E.: ‘Continuous phase modulation’, *IEEE Commun. Mag.*, 1986, **24**, (4), pp. 25–38
- Jones, A.E., Wilkinson, T.H., and Gardiner, J.G.: ‘Effects of modulator deficiencies and amplifier nonlinearities on the phase accuracy of GMSK signalling’, *IEE Proc., Commun.*, 1993, **140**, (4), pp. 157–163

- 19 Le, M.T., and Thibault, L.: 'Performance evaluation of COFDM for digital audio broadcasting – Part II: Effects of HPA nonlinearity', *IEEE Trans. Broadcast.*, 1998, **44**, (1), pp. 165–171
- 20 Chini, A., Wu, Y., El-Tanany, M., and Mahmoud, S.: 'Hardware nonlinearities in digital TV broadcasting using OFDM modulation', *IEEE Trans. Broadcast.*, 1998, **44**, (1), pp. 12–21
- 21 Mason, L.J.: 'Error probability evaluation for systems employing differential detection in a Rician fast fading environment and Gaussian noise', *IEEE Trans. Commun.*, 1987, **35**, (1), pp. 39–46
- 22 Makrakis, D., and Mathiopoulos, P.T.: 'Prediction/cancellation techniques for fading broadcasting channels – Part I: PSK signals', *IEEE Trans. Broadcast.*, 1990, **36**, (2), pp. 146–155
- 23 Makrakis, D., and Mathiopoulos, P.T.: 'Prediction/cancellation techniques for fading broadcasting channels – Part II: CPM signals', *IEEE Trans. Broadcast.*, 1990, **36**, (2), pp. 156–161
- 24 Makrakis, D., Mathiopoulos, P.T., and Bouras, D.P.: 'Optimal decoding of coded PSK and QAM signals in correlated fast fading channels and AWGN: A combined envelope, multiple differential and coherent detection approach', *IEEE Trans. Commun.*, 1994, **42**, (1), pp. 63–77
- 25 Toor, J.S.: 'Differentially detected GMSK systems in the presence of adjacent channel interference and nonlinearities', MSc dissertation, The University of British Columbia, Department of Electrical Engineering, Vancouver, 1994